

# Kinetic Study on Desulfurization of Hot Metal Using CaO and CaC<sub>2</sub>

DAVID LINDSTRÖM and DU SICHEN

The kinetics and reaction mechanisms of hot metal desulfurization using CaO and CaC<sub>2</sub> were studied in a well-controlled atmosphere with a lab scale high temperature furnace. The growths of CaS around CaO and CaC<sub>2</sub> were measured and compared at 1773 K (1500 °C). The parabolic rate constant was evaluated to be  $5 \times 10^{-7}$  (cm s<sup>-1</sup>) on CaO particles, and  $2.4 \times 10^{-7}$  (cm s<sup>-1</sup>) on CaC<sub>2</sub>. The bigger parabolic constant of CaO resulted in more efficient desulfurization. Agglomerates and big CaO particles led to 2CaO·SiO<sub>2</sub> formation which hindered further utilization of CaO for desulfurization. The 2CaO·SiO<sub>2</sub> formation was favoured by a high oxygen potential. Since the desulfurization reaction of CaO not only produced CaS but also oxygen, the local oxygen concentration around big CaO particles was higher than around small particles.

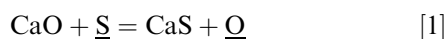
DOI: 10.1007/s11663-014-0195-8

© The Minerals, Metals & Materials Society and ASM International 2014

## I. INTRODUCTION

LIME and calcium carbide are two of the most commonly used agents for hot metal desulfurization. It is important to have a good understanding of their kinetics and reaction mechanisms to optimize material utilization. Although a number of studies<sup>[1–11]</sup> have been carried out, it is still difficult to compare the efficiencies of desulfurization using CaO and CaC<sub>2</sub>. The main reason is due to the scattered and even poor-defined experimental conditions.

The general view for hot metal desulfurization with CaO was described by Oeters.<sup>[7]</sup> Oeters reported that an outer layer of CaS together with 2CaO·SiO<sub>2</sub> was formed on the surface of CaO according to Reactions [1] and [2].



Reaction [1] proceeds by diffusion of the reactants (S and O) through the CaS layer whereas diffusion of reactants through the di-calcium silicate layer is slow and therefore, limits the desulfurization.<sup>[7]</sup>

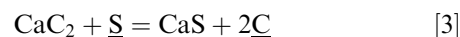
On the other hand, not only di-calcium silicate is formed around the CaO particle but also tri-calcium silicate.<sup>[9,10]</sup> It is argued that the addition of CaF<sub>2</sub><sup>[9]</sup> or Al<sup>[10]</sup> helps the formation of a slag layer around the CaO particle and thus increases the reaction rate.

Takahashi *et al.*<sup>[11]</sup> dipped CaO rods in hot metal with or without slag at 1723 K (1450 °C) under Ar-3 pctH<sub>2</sub>

gas atmosphere. No CaS formation on the CaO rod was observed in the absence of slag. They reasoned that solid CaO does not work at all for hot metal desulfurization because of the formation of silicate layer. They argue that CaO has to go into slag before it can have any effect on hot metal desulfurization.

On the other hand, Oeters *et al.* dipped sintered CaO rods in hot metal with and without silicon at 1573 K (1300 °C) and studied the growth of reaction products as a function of time.<sup>[6]</sup> A layer of 2CaO·SiO<sub>2</sub> was formed inside the outer layer of CaS when the hot metal contained silicon. CaS was the only reaction product in the experiments with silicon free hot metal. They concluded that solid state diffusion was the rate determining step at high sulfur concentrations whereas boundary layer diffusion was rate determining at lower sulfur concentrations.

In the case of calcium carbide used for hot metal desulfurization, a layer of CaS forms around the unreacted core of CaC<sub>2</sub> according to Reaction [3].<sup>[7]</sup>



Talballa *et al.*<sup>[8]</sup> observed a graphite layer formed between the CaS and CaC<sub>2</sub>. The authors speculated this carbon layer would slow down the desulfurization process.<sup>[8]</sup>

The contradicting observations reported in the literature are partly due to the difficulties in the experiments at high temperature and partly due to the different experimental conditions employed. The aim of the present work is to study the mechanisms of hot metal desulfurization using CaO and CaC<sub>2</sub> using a newly developed experimental setup. This setup ensures good controls of oxygen potential, temperature, addition of particles of CaO or CaC<sub>2</sub>, reaction time, and rapid quenching of the sample that allows the macroscopic examination of the reacted particles. In the light of mechanism study, the kinetics of desulfurization is also investigated.

DAVID LINDSTRÖM, Ph.D, Researcher, and DU SICHEN, Professor, are with the Department of Materials Science and Engineering, KTH Royal Institute of Technology, 10044 Stockholm, Sweden. Contact e-mail: sichen@kth.se

Manuscript submitted January 30, 2014.

Article published online September 25, 2014.

## II. EXPERIMENTAL

### A. Materials

All graphite parts were manufactured from IG10 high purity graphite. The hot metal used in this study was pig iron from a Swedish steel industry with an initial sulfur concentration of  $460 \pm 10$  ppm. The main composition of the hot metal is listed in Table I.

Fluidized lime powder was supplied by the company Lhoist and has the product name Flucal. The powder was surface-treated by silicon. The main component of the powder was CaO with  $<0.5$  mass pct  $\text{SiO}_2$  and traces of  $\text{CaF}_2$ . The size of the lime powder particles was estimated by size measurements of a large number of particles attached on a piece of tape observed with light optical microscope. Most particles were measured in the range between 50 and 100  $\mu\text{m}$ . In view of lime particles very often getting agglomerated during storage in the steel company, some lime powder was aged in a desiccator for a few months. Agglomerates (sizing a few hundreds of  $\mu\text{m}$ ) were formed in this type of CaO powder. Calcium carbide powder was obtained from SKW metallurgie group, with 80 pct of the particles being smaller than 63  $\mu\text{m}$ . The calcium carbide consisted of 95 mass pct technical  $\text{CaC}_2$  and 5 mass pct volatile

Table I. Main Components in the Hot Metal

	C	Si	S
Mass percent	3.9	0.21	0.046

coal. Note that a fraction of  $\text{CaC}_2$  had been transformed to  $\text{Ca}(\text{HO})_2$ .

### B. Setup and Procedure

A detailed description of the equipment can be found in a previous publication.<sup>[12]</sup> Only a salient feature of the setup is given here to orientate the readers. The experiment setup is presented in Figure 1.

The high temperature furnace with super Kanthal heating elements was controlled with a proportional integral differential (PID) controller using a B-type thermocouple (Pt-6 pctRh/Pt-30 pctRh). Another B-type thermocouple is placed just beneath the holding graphite crucible and allowed the sample temperature to be followed. The alumina reaction tube is connected to a water cooled quenching unit made of brass. The whole reaction chamber is gas tight by sealing with high temperature resistant rubber O-rings. To ensure efficient quenching of the sample, the quenching unit has two gas inlets that enable argon gas with a high flow rate to be flushed onto the sample when it is in the quenching position.

The hot metal is kept in a graphite crucible, which is held in graphite holder. A graphite connector connects the graphite holder to a long steel tube. The steel tube is placed in the central axial position and connected to the lift (Lift 1, driven by motor) above the reaction chamber. It is possible to slide the steel tube while at the same time ensuring good sealing using a system of rubber O-rings. Fast quenching is enabled by moving

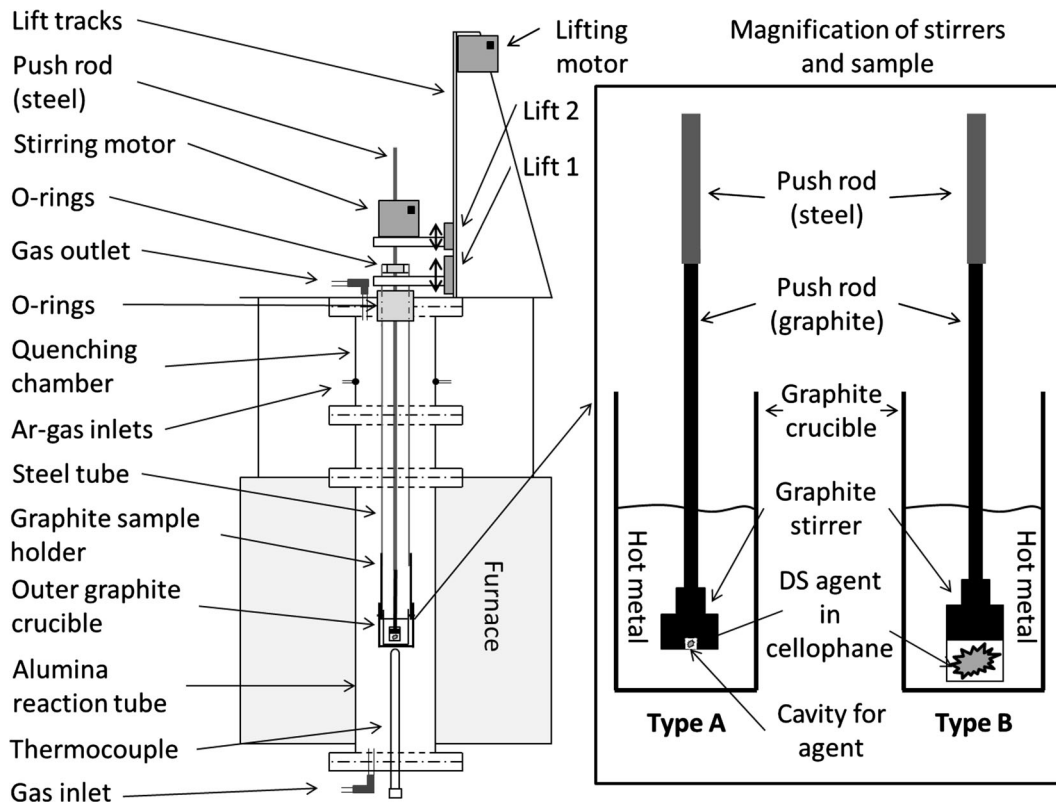


Fig. 1—The experimental setup.

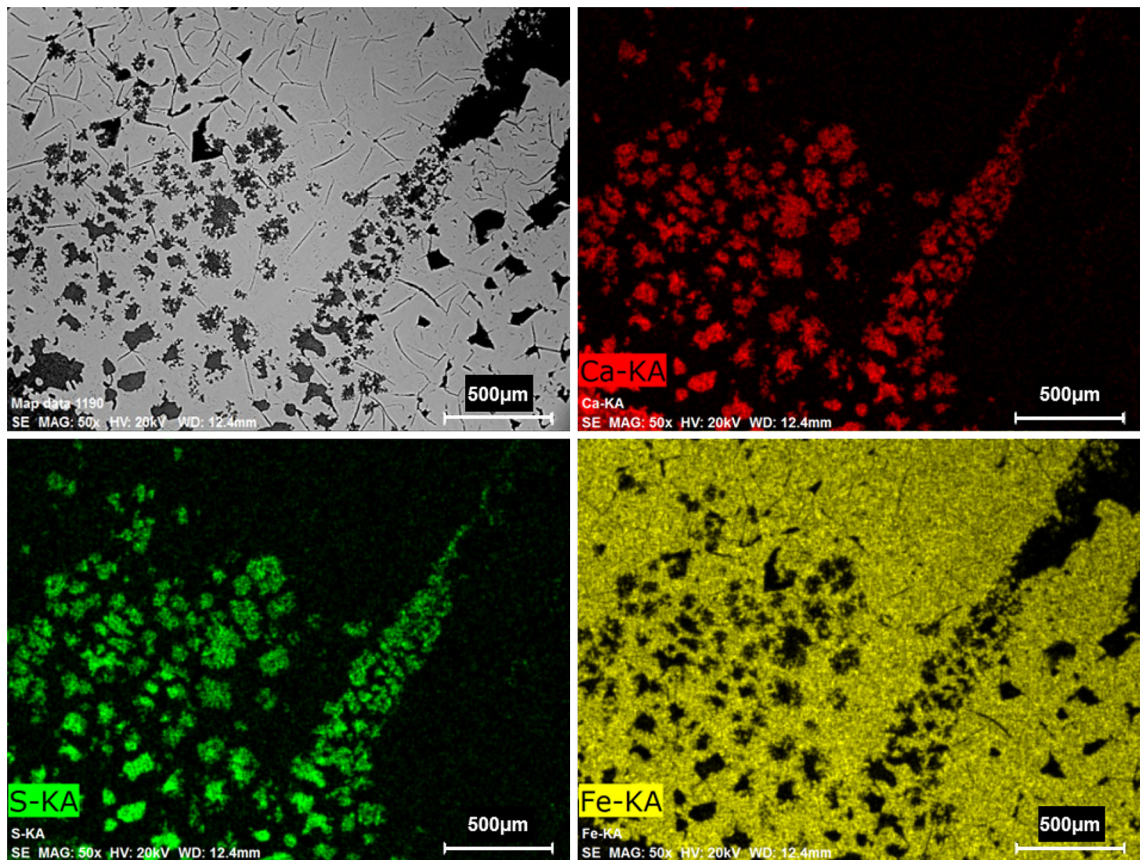


Fig. 2—Element mappings of CaO particles transformed to CaS in the hot metal bulk after 5 min.

the graphite holder from the hot zone of the furnace to the water cooled quenching unit in <1 second using the Lift 1.

A graphite push rod with a graphite impeller at the end is used for both stirring the metal bath and adding the reactant to the hot metal. The push rod is connected to a second lifting system (Lift 2) which makes it possible to move the graphite stirrer (and powder addition) both up and down relative to the first lifting system. The stirring motor (Eurostar Digital) which rotates the graphite impeller is placed on the platform also driven by Lift 2.

In all the experiments, pure CO gas was used. The reaction chamber was first evacuated and filled with argon 3 times at room temperature. Thereafter, the argon atmosphere was replaced by CO. CO gas at a low flow rate,  $0.02 \text{ L min}^{-1}$ , was used throughout the heating and reaction period. The use of CO and graphite would ensure the oxygen potential being at the same level of the hot metal reactor in the steel plant.

Two types of experiments were carried out, namely (i) study of the product layer on the added particle (CaO or CaC<sub>2</sub>) and its thickness as a function of time and (ii) determination of the degree of hot metal desulfurization as function of the added reactant quantity. In both cases 250 g of hot metal with an initial sulfur concentration  $460 \pm 10 \text{ ppm}$  (0.046 mass pct) was used.

Two different stirrers were employed for these two types of experiments. The details of the two graphite

stirrers are shown on the right side of Figure 1, marked as Type-A and Type-B, respectively. In the case of Type-A, a small cylindrical cavity (4 mm in depth and 8 mm in diameter) was made at the bottom of the stirrer. The addition of reactant was kept in the cavity by a small piece of very thin plastic cooking foil. In most experiments, an amount of 0.021 g powder was used, while in a few experiments with CaC<sub>2</sub> addition, a small cube of 0.023 g was used. All the CaC<sub>2</sub> samples were prepared in a dry box filled with argon. The calcium carbide cube was sized about  $2.1 \times 2.1 \times 2.1 \text{ mm}^3$  and grinded out of a bigger piece using 240# grit paper. Keeping the addition agent in the cavity would ascertain the reaction time and easy location of the reacted particles. In the experiment of Type-B, the powder of addition was wrapped at the tip of the graphite impeller with thin plastic foil.

In a typical run of Type-A experiment, the stirrer along with the desulfurization reagent was positioned in the cold zone of the reaction chamber, 1.4 m above the hot metal sample. The hot metal was heated up to 1773 K (1500 °C) and kept at there for 30 minutes for stabilization. Then, the stirrer with the reactant was quickly pushed down into the liquid metal; and stirring was started immediately. A stirring speed of 100 rpm was utilized for all experiments of this type. After a predetermined reaction time, the sample along with the stirrer was quickly moved to the quenching chamber (<1 second) by the lift and quenched by argon with high flow rate.

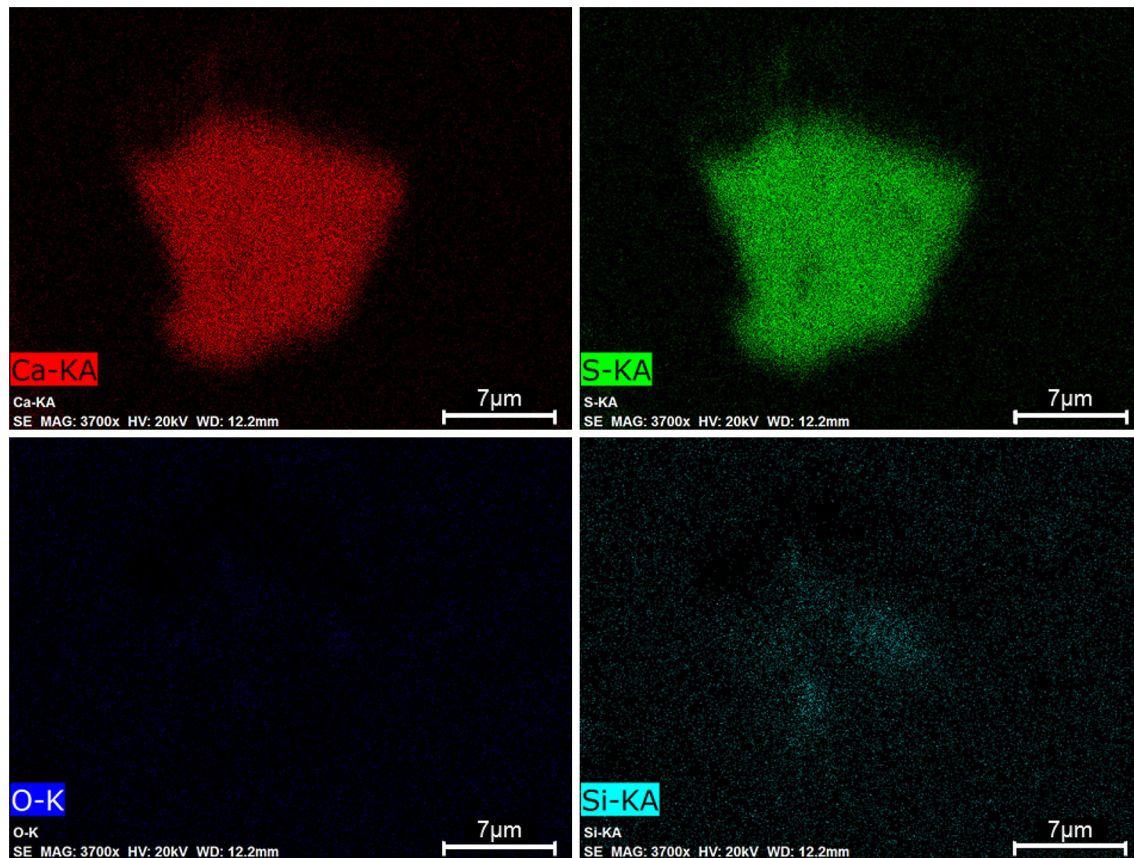


Fig. 3—CaO (Flucal) particle completely converted to CaS shown by element mappings.

A cutting machine was used to prepare cross-sections of the sample. Special effort was taken to get the cross-section through the lime or calcium carbide particles. High purity ethanol (99.8 pct) was used to clean the surface directly after cutting. Ethanol was also used as cooling agent during grinding and polishing of the surface of the cross-section. Great care was taken to minimize influence of the preparation procedure on the reacted particles. To study the reaction, the particles were examined using a Hitachi S-3700 scanning electron microscope equipped with EDS. Sometimes a Leica light optical microscope was also employed.

In a typical run of Type-B experiment, a carefully weighed amount of the reactant powder (Flucal or  $\text{CaC}_2$ ) was wrapped to the tip of the graphite stirrer using a piece of very thin plastic foil (Figure 1). The graphite stirrer along with the reactant was then positioned in a cold part of the reaction chamber 1.4 m above the hot metal sample. The hot metal was heated up to 1773 K (1500 °C) in an atmosphere of pure CO and kept at this temperature for 30 minutes. The stirrer with the reactant powder was quickly pushed into the hot metal with the pushrod. Immediately after the addition of the reactant, stirring was started using the stirring motor. In order to compare the rate of desulfurization of the reactants, the same stirring conditions were employed for all runs, *viz.* the hot metal was stirred by the impeller at 400 rpm for 5 minutes. Thereafter, the stirrer was lifted out of the hot metal and the sample was

kept in this position for 5 minutes so that reaction products could float to the top of the sample before quenching. The sample was then lifted up to the quenching chamber (in <1 second) and quenched by Ar-gas at very high flow rate.

The hot metal samples after the Type-B experiment were sent for chemical analysis (C, Si, and S). In general, the hot metal after the experiments contained 5.4 mass pct C and 0.25 mass pct Si. The sulfur analysis was carried out using LECO combustion analysis (ASTM E1019).

### III. RESULTS

#### A. Mechanisms of the Reactions (Type-A Experiments)

##### 1. CaO (fluidized lime)

Different reaction times were used in the experiments. When the reaction time is long enough, most of the single particles (most particles were measured in the range between 50 and 100  $\mu\text{m}$ ) are transformed to CaS.

Figure 2 presents the element mappings over a cross-section of the sample quenched 5 minutes after the Flucal addition. It is clearly seen that almost all the CaO particles have been completely transformed into CaS. Figure 3 presents a particle converted from CaO to CaS completely at high magnification. It is interesting to see that no silicon is present around the particle, indicating thereby the absence of any calcium silicate layer.

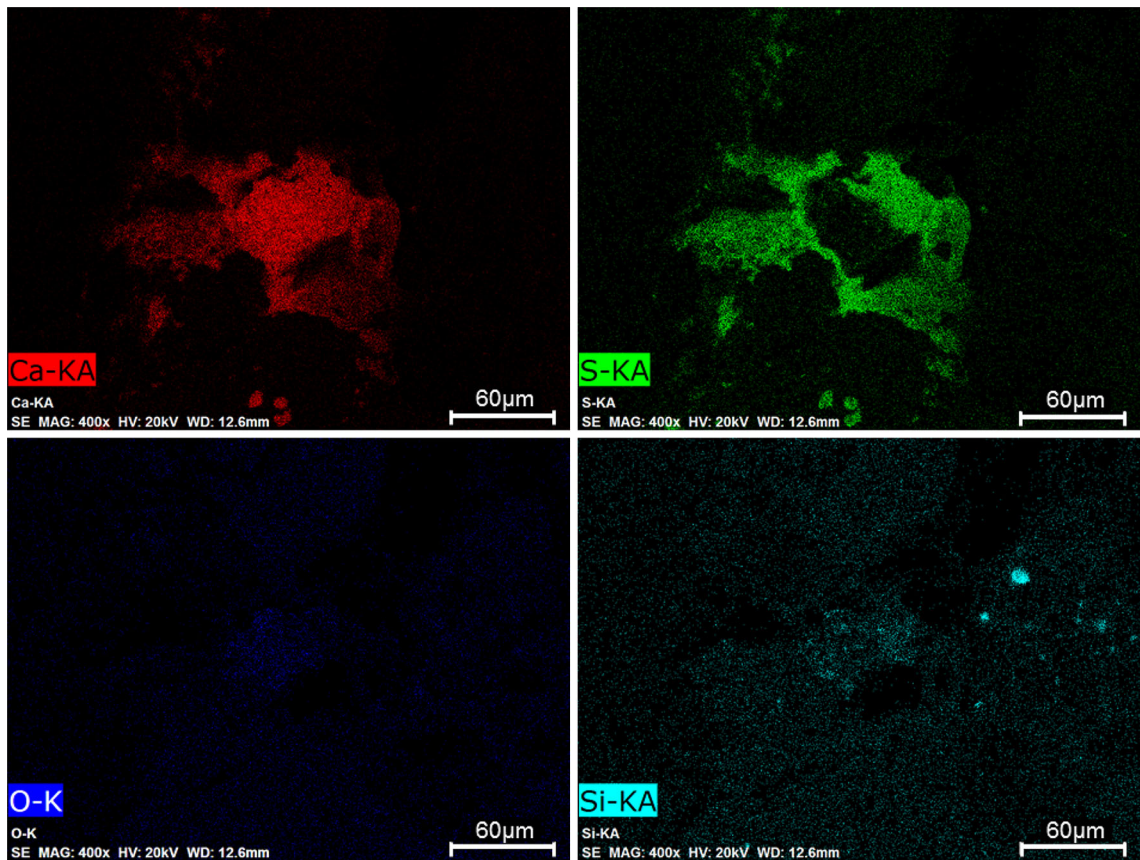


Fig. 4—Element mappings showing a CaS layer formed around a CaO particle after 30 s.

When the reaction time is short, a layer of CaS is formed on the surface of the CaO particle. The element mappings of a particle reacted for 30 seconds are presented in Figure 4. The mappings clearly show the CaS layer. The particle is about 100  $\mu\text{m}$ , while the CaS layer is about 30  $\mu\text{m}$ . Similar to the particles shown in Figure 3, the absence of calcium silicate layer is evident.

The thickness of the CaS on the surface of Flucal particle is presented as function of reaction time in Figure 5. Note that all measurements of the CaS layer using SEM are carried out only on single particles. Because of the difficulties in polishing a sample that consists of materials having very different harnesses, some part of the CaS layer is unavoidably removed during sample preparation. Hence, it is believed that the thickest part would represent the layer better. The values plotted in Figure 5 are the average values of a number of measurements.

Figure 6 presents the element mappings of the sample quenched after 5 minutes of reaction time. It shows the presence of calcium silicate. EDS analysis suggests that both  $3\text{CaO}\cdot\text{SiO}_2$  and  $2\text{CaO}\cdot\text{SiO}_2$  are present. Note that the formation of calcium silicate phases is only observed in big agglomerates. Note that in this type of experiments, aged lime powder was used. The agglomerate shown in figure is about 500 to 600  $\mu\text{m}$ . The presence of CaS and calcium silicate is evident. The formation of calcium silicate will be discussed in detail later in the discussion part.

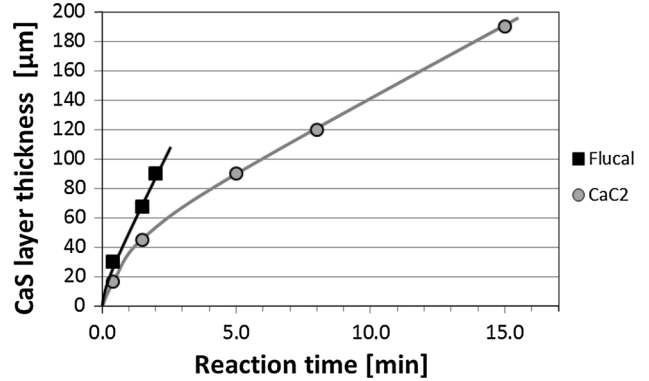


Fig. 5—CaS layer thickness as a function of time measured on single CaO particles and  $\text{CaC}_2$  cubes.

## 2. Calcium carbide

Figure 7 shows the element mappings of a calcium carbide particle with a diameter of approximately 25  $\mu\text{m}$  after reaction of 25 seconds. An outer layer (about 10  $\mu\text{m}$  in thickness) of CaS is formed around the unreacted carbide. It should be mentioned that the carbon mapping is not presented in figure due to the great uncertainties associate with carbon analysis using EDS. The absence of calcium silicate phase is also evidently shown.

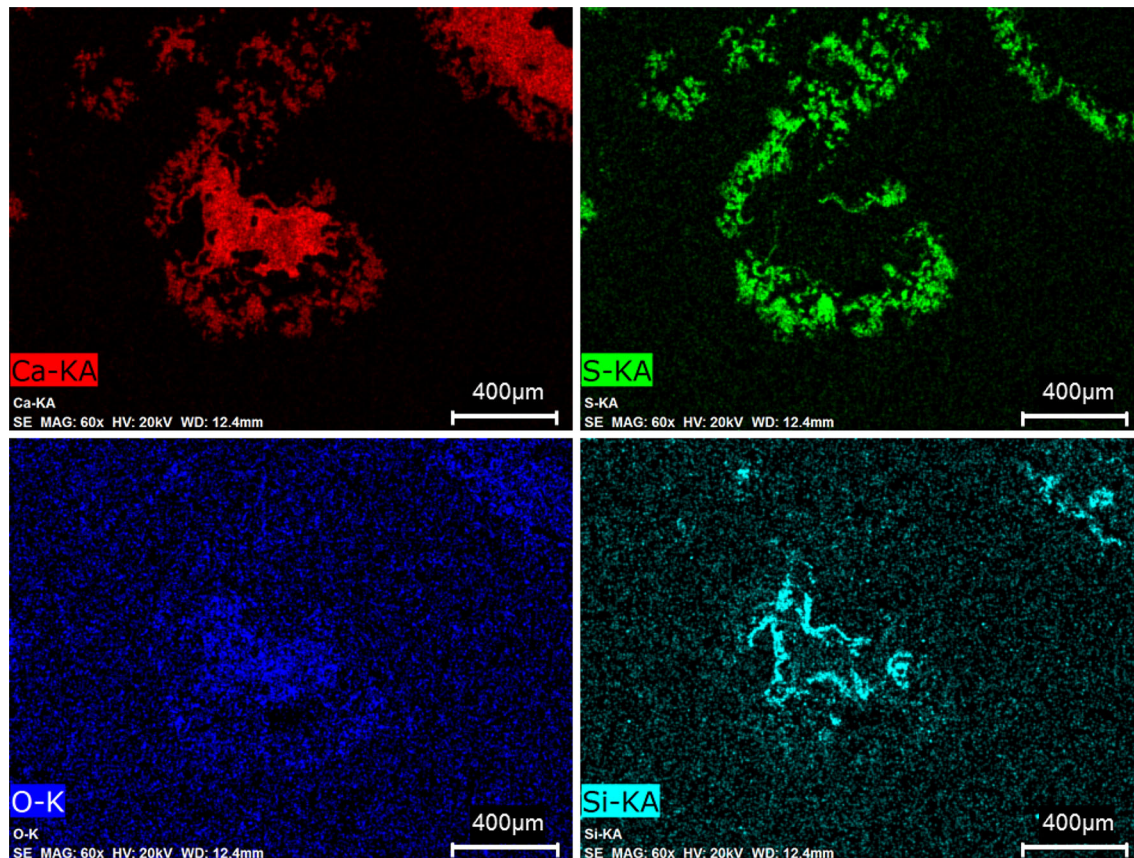


Fig. 6—A layer of di-calcium silicate formed inside the CaS layer on a big lime agglomerate (shown by element mappings).

Figure 8 presents the element mappings over the cross-section of the calcium carbide cube quenched after 8 minutes of reaction. A thick layer of CaS about 120  $\mu\text{m}$  in thickness was formed around the calcium carbide cube. Between the CaS layer and the remaining  $\text{CaC}_2$  cube, a thin graphite layer is detected. Although the carbon analysis using EDS involves great uncertainty, the absence of Ca in this layer is a strong evidence of the layer of graphite phase. Note that the upper part of the remaining  $\text{CaC}_2$  has been lost during polishing. The graphite layer was also reported by Talbala *et al.*<sup>[8]</sup> The CaS outer layer grows inward from the original interface between hot metal and calcium carbide. It is worthwhile to mention that the silicon mapping evidently indicates the absence of any calcium silicate phase.

The thickness of CaS layer as a function of reaction time is also presented in Figure 5. In view that the layer thickness measured in the  $\text{CaC}_2$  particle compares well with the measurements in cubes at lower reaction times, the layer thickness at longer reaction times are measured using cubes (The  $\text{CaC}_2$  particles are smaller than 100  $\mu\text{m}$ ).

#### B. Degree of Desulfurization (Type-B Experiments)

Different amounts of either fluidized lime powder or  $\text{CaC}_2$  powder were added to the hot metal to study the degree of desulfurization. In order to compare the results in a systematic manner, the amount of hot metal, the initial sulfur content in the hot metal, the stirring speed, and time were all kept the same for all experi-

ments in this series. The experimental conditions are summarized in Table II.

The added moles of Flucal or calcium carbide were varied from 1 to 7 times of the moles of sulfur originally in the hot metal. The amount of reactant added is expressed as:

$$N_{\text{add}}^i = \frac{n_i}{n_s} \quad [4]$$

where the subscript  $i$  stands for either CaO or  $\text{CaC}_2$ . In Eq. [4],  $n_s$  denotes the initial number of moles of sulfur in the hot metal.

Figure 9 presents the analyzed sulfur level in the sample after the experiment as a function of  $N_{\text{add}}^i$ . Figure shows a clear trend for both Flucal and calcium carbide, that a larger amount of addition leads to a lower final sulfur level. As shown in figure, with  $N_{\text{add}}^i = 3.5$ , Flucal reduces the sulfur content from 460 to 40 ppm, while  $\text{CaC}_2$  to 230 ppm. At  $N_{\text{add}}^i = 7$ , while the sulfur content after  $\text{CaC}_2$  addition is still high, Flucal reduces it to <20 ppm.

## IV. DISCUSSION

#### A. Formation of Calcium Silicate

The formation of calcium silicate layer on the surface of CaO has been reported by a number of researchers when hot metal contains silicon.<sup>[3,6,7,9–11]</sup> Takahashi

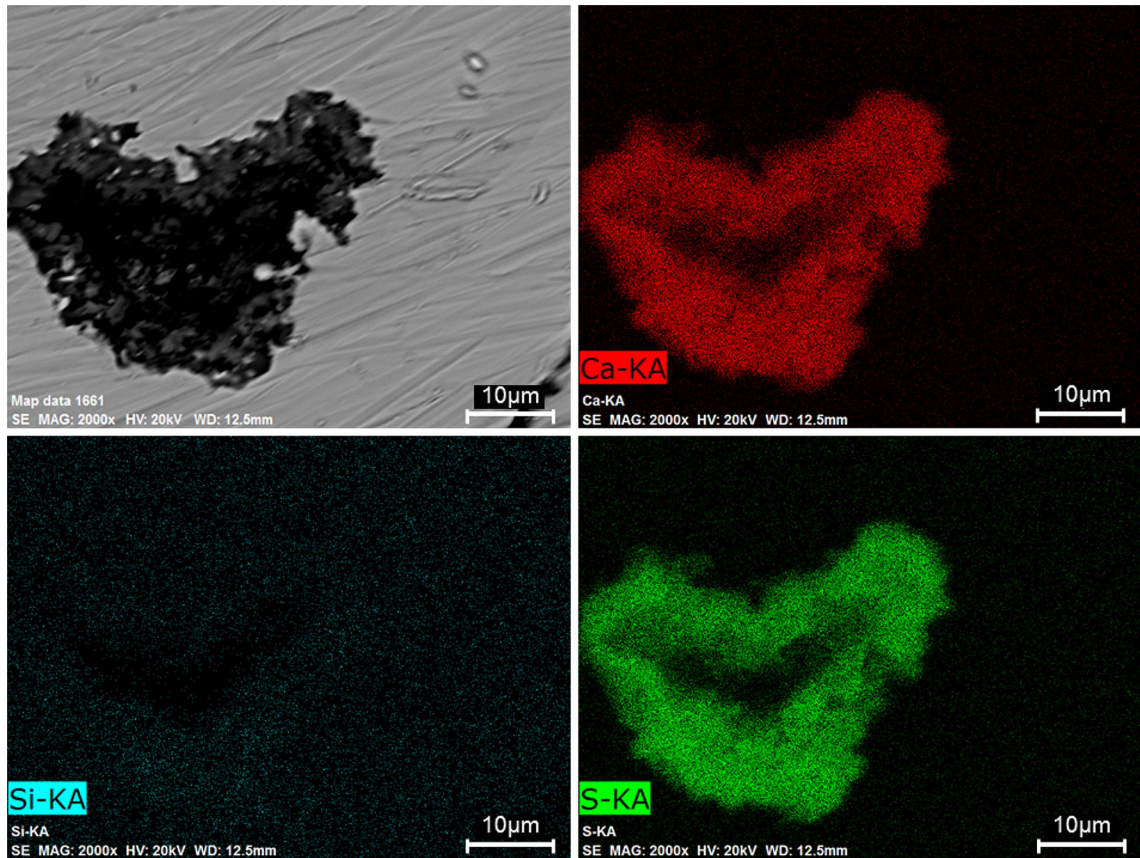
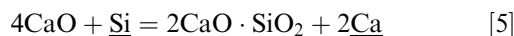


Fig. 7—CaS layer around a CaC<sub>2</sub> particle and the absence of silicates is shown by element mappings.

*et al.*<sup>[11]</sup> even claim that a micro slag layer has to be present around solid lime in order for significant CaS formation to take place. The present observation is in contradiction to Takahashi's reasoning. As shown in Figures 3, 4, 7 and 8, CaS layer is formed on the surface of both CaO and CaC<sub>2</sub>, while no calcium silicate is detected. Figure 9 shows that the desulfurization can be very efficient by fluidized lime particles. Even CaC<sub>2</sub> works to great extent in desulfurization.

Oeters *et al.*<sup>[6]</sup> reported that a layer of 2CaO·SiO<sub>2</sub> was formed inside the outer layer of CaS when the hot metal contained silicon. On the other hand, no silicate layer is detected in the small fluidized lime particles. In contrast with the small oxide particles, calcium silicate is found in the agglomerates in the present study as shown in Figure 6. In agreement with Oeters' observation, the calcium silicate layer is inside the CaS layer. It should be mentioned that Oeters *et al.*<sup>[6]</sup> used CaO rods in their study. Their results along with Figure 6 suggest that a bigger mass of CaO is needed to create the calcium silicate layer.

There are two possible reaction routes for di-calcium silicate to form, *viz.*



and



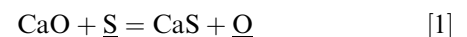
The underlined letters means that these elements are dissolved in liquid iron. It is well known that the con-

centration of dissolved Ca in hot metal is extremely low, typically below 1 ppm. This low solubility would make the mass transfer of Ca extremely slow due to the low driving force, *viz.*  $\Delta([\text{mass percent Ca}]_{\text{interface}} - [\text{mass percent Ca}]_{\text{hot-metal}}) < 1 \text{ ppm}$ , since the mass transfer rate is proportional to this driving force,

$$\dot{m} = AkA([\text{mass percent Ca}]_{\text{interface}} - [\text{mass percent Ca}]_{\text{hot-metal}}) \quad [6]$$

where  $k$  is the mass transfer coefficient and  $A$  is the interfacial area. The extremely small concentration gradient of dissolved calcium would rule out practically the possibility of calcium supply for Reaction [5].

Since most of the hot metal contains considerably high concentration of dissolved silicon and CaO is added as the desulfurization agent, the limiting factor for the formation of calcium silicate through Reaction [2] would be the oxygen supply. It is well known that the oxygen level in hot metal is at ppm level, which will not be enough to generate calcium silicate. This argument is supported by the absence of calcium silicate in the case of single small fluidized lime particles (Figures 2 and 3). The desulfurization reaction,



leads to the formation of oxygen.

However, a tiny CaO particle (usually  $< 50 \mu\text{m}$ ) is converted completely to CaS before the calcium silicate

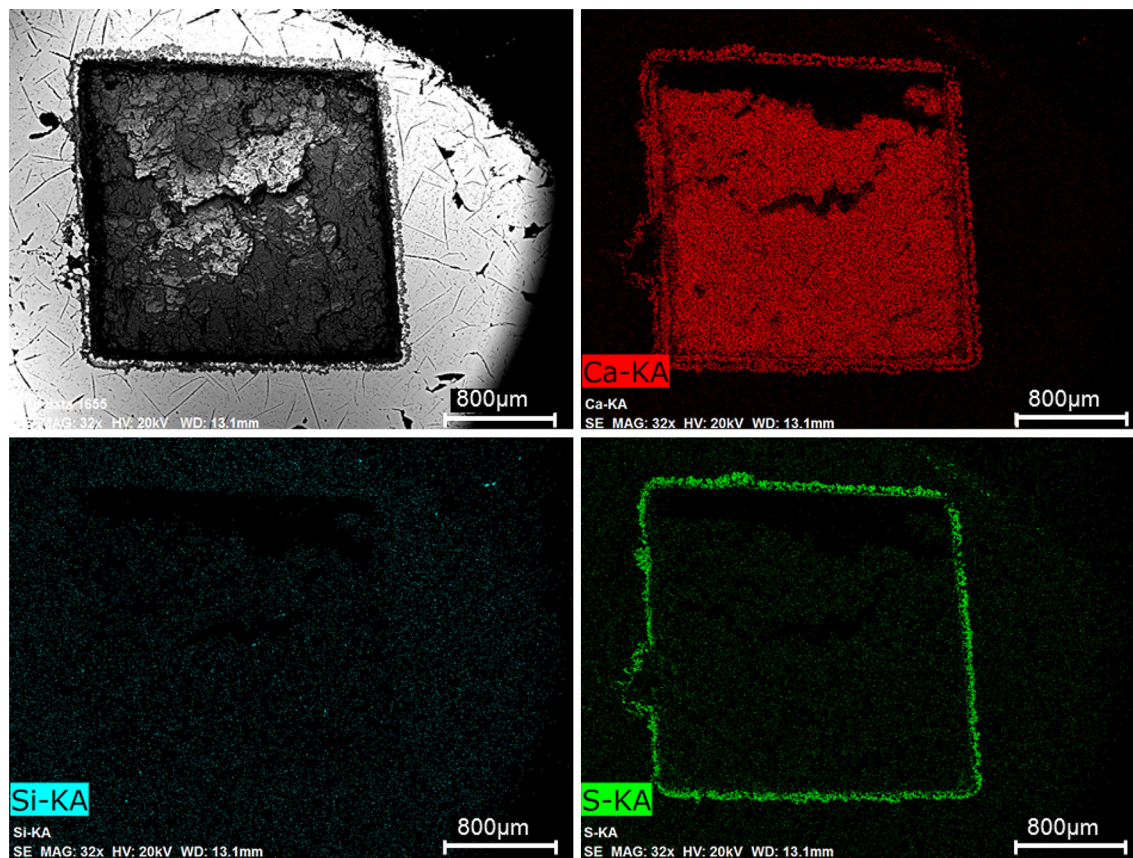


Fig. 8—Element mappings of cross-section of a  $\text{CaC}_2$  cube showing the CaS layer after 8 min.

**Table II. Experimental Conditions Used During Type-B Experiments**

Hot Metal (g)	Initial $\underline{\text{S}}$ (ppm)	Stirring Speed (rpm)	Stirring Time (min)	Flotation Time (min)
250.00	460	400	5	5

The underlined letters means that these elements are dissolved in liquid iron.

layer has formed (see Figure 3). This is a direct observation in the experiments. It is the result of both kinetics and thermodynamics. In the case of bigger particles or CaO agglomerates, the silicate layer is formed when the layer of CaS has become thicker (*e.g.*, 40  $\mu\text{m}$ ). The increase of the local oxygen potential at the CaS–CaO interface would result in the formation of calcium silicate under the thick CaS layer, as observed in the present experiment (see Figure 6). This reasoning is also valid for the experiments using CaO rods. This explains why in all the experiments using CaO rods,<sup>[6,11]</sup> calcium silicate is always detected.

It is expected, therefore, that massive addition of CaO locally would lead to fast formation of calcium silicate phase and therefore increase the resistance for mass transfer (diffusion through the calcium silicate layer). The formation of the calcium silicate phase would not only slow down the desulfurization process, but also reduce the efficiency of the agent. As seen in Figure 6, a great fraction of the agglomerate is still CaO. The formation of calcium silicate would also take place when big piece of CaO is employed, which is demonstrated in the literature<sup>[10]</sup> and

also in Figure 6. Note that since the metal bath was stirred by impeller, the mass transfer in the liquid is quit fast in the present experiments. The mass transfer in the industrial reactor might be very much different. Hence, the discussion about the formation of  $2\text{CaO}\cdot\text{SiO}_2$  layer should be considered qualitative. To minimize or even avoid the formation of calcium silicate phase, using tiny particles is desired. It is also desired that the tiny particles are dispersed well in the hot metal, so that the local oxygen concentration would not result in substantial amount of oxygen through Reaction [1]. Addition of Flucal-Mg mixture seems to be a promising alternative. As reported in the previous work,<sup>[12]</sup> Mg generates huge amount of Mg-gas, which helps greatly in dispersing the CaO tiny particles. The presence of Mg will also reduce the oxygen level in the locations of CaO addition by the following reaction:



Good particle dispersion and low oxygen level will minimize the formation of calcium silicate and increase the efficiency of desulfurization.



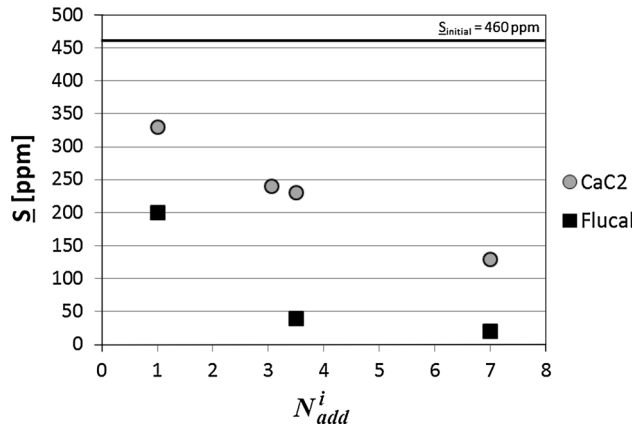
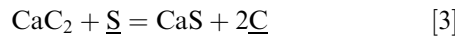


Fig. 9—Sulfur concentration in metal after desulfurization as a function of added quantity.

The above discussion is further supported by the absence of calcium silicate in the case of  $\text{CaC}_2$  (see Figures 7 and 8). The desulfurization by  $\text{CaC}_2$  can be expressed as:



Since no oxygen is generated, calcium silicate cannot be formed.

Both  $2\text{CaO}\cdot\text{SiO}_2$  and  $3\text{CaO}\cdot\text{SiO}_2$  are found in the agglomerates after the experiments, though it is hard to quantify their fractions. It seems that  $3\text{CaO}\cdot\text{SiO}_2$  exists close to  $\text{CaO}$  due to the higher  $\text{CaO}$  activity.  $2\text{CaO}\cdot\text{SiO}_2$  is found near the  $\text{CaS}$  layer. However, it is very difficult to illustrate this aspect because of the particles in the agglomerates are so small.

### B. Desulfurization Without Calcium Silicate Layer

As discussed above, it is possible to use tiny and dispersed  $\text{CaO}$  particles (*e.g.*, Flucal) to desulfurize the hot metal without the formation of calcium silicate layer. In fact, the calcium silicate layer does not exist in the case of  $\text{CaC}_2$  desulfurization.

As seen in the SEM microphotographs (Figures 4 and 8), in the absence of calcium silicate layer, the desulfurization proceeds by diffusion through the  $\text{CaS}$  phase in the case of  $\text{CaO}$  and by diffusion through both  $\text{CaS}$  layer and graphite layer in the case of  $\text{CaC}_2$ . In the present experiments of Type-A, <10 pct of the amount of reactant needed for complete desulfurization is used. The hot metal bath is constantly stirred at 100 RPM. It is expected that the mass transfer in the liquid phase would not be limiting kinetic factor.

The reaction rate can, therefore, be considered inversely proportional to the instantaneous reaction product layer thickness according to Eq. [8].

$$\frac{dx}{dt} = \frac{K}{x} \quad [8]$$

where  $x$  is the  $\text{CaS}$  layer thickness,  $t$  is the reaction time, and  $K$  is the parabolic rate constant. On integration, Eq. [8] leads to

$$x = \sqrt{2Kt} \quad [9]$$

An evaluation of the parabolic rate constants for these two cases would throw some lights on the performances of the two types of materials. The parabolic rate constants,  $K$ , for  $\text{CaO}$  and  $\text{CaC}_2$  are calculated using Eq. [9] based on the data in Figure 5. The parabolic rate constant is calculated to be  $2.4 \times 10^{-7} \text{ (cm s}^{-1}\text{)}$  for calcium carbide and  $5 \times 10^{-7} \text{ (cm s}^{-1}\text{)}$  for fluidized lime. It should be mentioned that experimental data for  $\text{CaC}_2$  include both particle and cube data, since they are comparable. It is not proper to make cube for Flucal, as the product utilizes the advantage of surface treatment. The use of cube would lead to misleading results. Oeters *et al.*<sup>[6]</sup> reported  $\text{CaS}$  growth on dense lime rods exposed to hot metal as a function of time at 1573 K (1300 °C). Using this data, a  $K$  value of  $1.8 \times 10^{-9} \text{ (cm s}^{-1}\text{)}$  is calculated. The value is much lower than the present one. While the lower temperature of their study would be one of the reasons for their low  $K$ , the difference of the surface properties could be the more reasonable explanation since Flucal particles are specially treated. Also the formation of calcium silicate layer would create another resistance in addition of the  $\text{CaS}$  layer. This calcium silicate layer would slow down the growth of  $\text{CaS}$ .

The doubled  $K$  value of fluidized lime in comparison with  $\text{CaC}_2$  well explains the high efficiency of the particles in desulfurization as shown in Figure 9.

It should be mentioned that the experiments are carried out in a reducing environment, while in the real industrial environment the melt is usually surrounded by ambient air. However, in view that the desulfurization reaction would take place either in the liquid bath or/and at the slag-metal interface, the oxygen potential in the hot metal would be the dominant factor. The oxygen potential at the reaction sites in the reactor would be very similar as the present condition.

The present results reveal that fluidized  $\text{CaO}$  particles are very efficient in desulfurization in comparison with  $\text{CaC}_2$ . This is because of the lower diffusion resistance of  $\text{CaS}$  layer formed on the particle surface. To keep this advantage, avoiding the agglomeration of the particles and therefore the formation of calcium silicate layer is essential. Adding the powder in an optimized manner will help the dispersion of the particle in the liquid metal. Addition of Flucal-Mg mixture would be in line with this reasoning. The presence of Mg can even lower the oxygen generated by Reaction [1] and further minimize the formation of calcium silicate phase.

## V. SUMMARY

The kinetics and reaction mechanisms of hot metal desulfurization by  $\text{CaO}$  and  $\text{CaC}_2$  were studied at 1773 K (1500 °C) in a newly designed experimental setup. The setup had good control of oxygen potential and the ability to quench the sample.

No silicate formation was found in the case of  $\text{CaC}_2$ ; but a layer of carbon is formed between the  $\text{CaS}$  layer and  $\text{CaC}_2$ . In the case of  $\text{CaO}$ , small particles (<50  $\mu\text{m}$ ) were completely transformed into  $\text{CaS}$ . When the  $\text{CaO}$  particles were big or had formed agglomerates, the local oxygen concentration at the interface of  $\text{CaS}$  and  $\text{CaO}$  increased

during desulfurization and, therefore, favoured the formation of  $2\text{CaO}\cdot\text{SiO}_2$ . The  $2\text{CaO}\cdot\text{SiO}_2$  layer was formed between the CaS layer and CaO. This layer acted as a second resistance hindering the diffusion of reactants for further utilization of the CaO for desulfurization. Hence, big CaO particles and/or agglomerates of lime particles must be avoided to ensure a high efficiency of the lime agent for desulfurization. Small additions of Mg would provide a possibility to achieve this goal because the rapid formation of Mg-gas could help spreading the lime particles.

The parabolic reaction rate constants were calculated to be  $2.4 \times 10^{-7}$  ( $\text{cm s}^{-1}$ ) for  $\text{CaC}_2$  and  $5 \times 10^{-7}$  ( $\text{cm s}^{-1}$ ) for CaO (Flucal). The higher value of CaO was in accordance with the higher efficiency of CaO in desulfurization.

#### ACKNOWLEDGMENT

The financial support from Lhoist is gratefully acknowledged.

#### REFERENCES

1. G.A. Irons: *Ironmak. Steelmak.*, 1989, vol. 16, pp. 28–36.
2. C.F. Landefeld: *Process technology proceedings, vol. 6, Book 3, 5th International Iron and Steel Congress*, Iron and Steel Society, Washington, DC, 1986, pp. 411–18.
3. Y. Kawai, K. Mori, and Y. San-Nomiya: *Tetsu-to-Hagane*, 1975, vol. 61, pp. 29–35.
4. D.C. Boyd, W.C. Phelps, and M.T. Hepworth: *Metall. Trans. B*, 1975, vol. 6B, pp. 87–93.
5. M. Ueda, Y. Fujita, K. Nakai, T. Toshimori, and Z. Morita: *Tetsu-to-Hagane*, 1989, vol. 75, pp. 58–65.
6. F. Oeters, P. Strohmenger, and W. Pluschkell: *Arch. Eisenhüttenwes.*, 1973, vol. 44, pp. 727–33.
7. F. Oeters: *Steel Res.*, 1985, vol. 56, pp. 69–74.
8. M. Talbala, P.K. Tojan, W.C. Bigelow, R.A. Flinn, and L.O. Brockway: *AFS Trans.*, 1976, vol. 84, pp. 775–86.
9. C.F. Landefeld and S. Katz: *Process technology proceedings, vol. 6, Book 3, 5th International Iron and Steel Congress*, Iron and Steel Society, Washington, DC, 1986, pp. 429–39.
10. T. Shoji, T. Mitsuo, Y. Hatta, H. Ono, H. Mori, and T. Kai: *Tetsu-to-Hagane*, 1982, vol. 68, pp. 609–17.
11. K. Takahashi, K. Utagawa, H. Shibata, S. Kitamura, N. Kikuchi, and Y. Kishimoto: *ISIJ Int.*, 2012, vol. 52, pp. 10–17.
12. D. Lindström, P. Nortier, and D. Sichen: *Steel Res. Int.*, 2014, vol. 85, pp. 76–88.